Predicting self-assembly and structure in diluted aqueous solutions of modified mono- and bis-β-cyclodextrins that contain naphthoxy chromophore groups

UNIVERSITÀ DEGLI STUDI DI TORINO

Predicting self-assembly and structure in diluted aqueous solutions of modified *mono*- and *bis*-βcyclodextrins that contain naphthoxy chromophore groups

Thais Carmona[a], Katia Martina[b], Laura Rinaldi[b], Luisa Boffa[b], Giancarlo Cravotto[b], Francisco Mendicuti[a]*

The water diluted solution behaviour of *mono*- and *bis*-βciclodextrin derivatives (*mono*- and *bis*-CD), whose appended groups and inter-CD linkers contain a naphthoxy chromophore moiety, has been studied using steady-state and time-resolved fluorescence techniques, circular dichroism and Molecular Modelling. *Mono*-CD derivatives form non-covalent dimeric tail-to-tail supramolecular structures via the mutual partial penetration, through their primary sides, of *axially* oriented naphthoxy appended groups and the self-inclusion of the naphthoxy moiety is rather improbable. Non-covalent dimer formation may compete with any guest complexation. Nevertheless, these assemblies can be broken up by decreasing medium polarity or when the appended group is captured by macrorings such as cucurbit[7]urils or native βCDs. *Bis*-CD derivatives, however, do not exhibit self-association processes which were observed in the *mono*-derivatives. This is because the presence of the bulky naphthoxy group in the spacer keeps the βCD cavities, which are capable of accommodating an external guest, away from each other. The dinaphthoxy group, in the *bis*-NβCD, was located in a quasi-parallel plane conformation between both CDs.

Introduction

Cyclodextrins (CDs) are cyclic hollow oligosaccharides composed of α-(1→4)-linked glucopyranosyde units and are used as host molecules in supramolecular chemistry. They are able to include guest molecules of an appropriate size and thereby act as molecular containers.[1, 2] CDs present two well differentiated hydrophilic primary and secondary faces, to which hydroxyl groups are attached, and a hydrophobic inner cavity. Complexation of any guest in water means that the polarity and microviscosity of the surrounding medium substantially varies. These changes influence guest chromophore spectroscopic properties, allowing the thermodynamics and the structure of the complex to be studied.[3-11] A chromophore can be covalently attached to a βCD macroring in order to obtain fluorescent *mono*-CD derivative hosts. Appended groups are capable of hindering or favouring the complexation of guests, or even modifying their capabilities for aggregation into dimers, according to their shape, size and flexibility of the link to the core of the molecule.[10, 12-30] *Mono*-CDs have been extensively investigated in a number of roles, including light harvesting host molecules,[13, 31-33] building blocks for functional supramolecular architectures,[30, 34, 35] catalysts[36] and in sensing applications.[37-39]

Attaching another CD to the end of the appended moiety resulted in *bis*-CD derivatives. Cooperation between the CDs and spacer-guest interactions improve *bis*-CD recognition and sensing capabilities.[40-68]

The copper-catalyzed azide-alkyne cycloaddition protocol (CuAAC) is a powerful method for the preparation of CD derivatives. In a relatively recent work, Cravotto et al. applied this technique for the preparation of homo- and heterodimers, as well as CD oligomers whose linkers contained 1,2,3-triazole groups.[69-71] Our group has reported the in solution behaviour of some *mono*- and *bis*-βCD derivatives, which were also prepared using CuAAC, whose appended groups or linkers between βCDs contained the 1,3-diphenoxy chromophore moiety. [29] The use of circular dichroism in conjunction with MD simulations allowed us to obtain information on the structure of both derivatives in water solution. Self-inclusion of the appended moiety for *mono*- or *bis*-βCDs was discharged. Nevertheless, the *mono*-βCD was capable of forming very stable dimer and oligomer structures in water, where diphenoxy groups, *axially* oriented in relation to the main CD axis, were partially located outside the cavity. The *bis*-βCD, however, maintain a rather open arrangement where both CD macrorings are relatively distant and parallel. We subsequently discovered[68] that a strong *mono*-βCD association hindered complexation with a naphthalene dicarboxylate fluorescence probe (DMN)[72] which is not capable of breaking strong supramolecular structures. However, DMN gave 1:1 and 2:1 stoichiometry complexes with *bis*-βCD. Cooperativity between CDs improved binding capability, relative to the DMN:βCD complex, by a factor of 7.[72]

The present work aims to predict the structures of modified βCDs, that contain naphthoxy chromophore groups, in diluted water solution. These modified βCDs are namely 6^{I}-deoxy-6^{I}-(4-((2-naphthyloxy)methyl)-1*H*-1,2,3-triazol-1-yl)-β-cyclodextrin (*mono*-NβCD) and 2,7-bis-((1-(6^{I}-deoxy-β-cyclodextrin-6^{I}-yl)-1*H*-1,2,3-triazol-4-yl)methoxy)naphthalene, (*bis*-NβCD). A combination of steady-state and time-resolved fluorescence techniques, Induced Circular Dichroism (ICD) measurements and Molecular Mechanics and Molecular Dynamics (MD) calculations were used for this purpose. The complexation of 2-Metiloxynaphtalene, (MON) and 2,7-dimethoxynaphthalene (dMON), chromophoric model compounds, with native βCD were also studied [Fig. 1]. Overall results have permitted us to hypothesize the structure of these modified CDs in a diluted aqueous solution. These results will be useful in dealing with the complexation of adducts that contain Gd(III) chelates, which have applications as contrast agents (CAs) for MRI diagnosis.[71] This will be one of our main objectives for subsequent studies.

[a] *Departamento de Química Analítica, Química Física e Ingeniería Química, Universidad de Alcalá. 28871 Alcalá de Henares. Madrid. Spain. E-mail: francisco.mendicuti@uah.es*

b Dipartimento di Scienza e Tecnologia del Farmaco of the University of Torino. Via Pietro Giuria, 9-10125 Torino, Italy.

† Electronic supplementary information (ESI) available: Synthesis Protocols, Characterization and additional figures: Fig. 1S-8S and Tables 1S-3S. See DOI: 10.1039/b000000x/

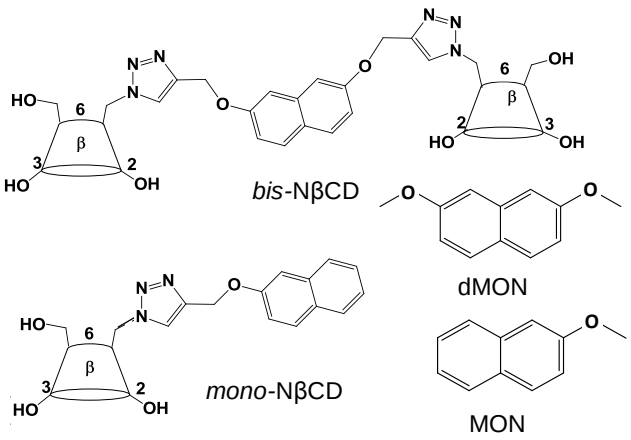

Fig. 1 Structures of the modified CDs and model compounds studied.

Results and Discussion

The naphtoxy chromophore group was bound to the βCD core by Cu(I)-catalyzed Huisgen 1,3-dipolar cycloaddition using metallic copper under sonochemical conditions [Schemes 1 and 2, ESI].[73] 6^{I}-Azido-6^{I}-deoxy-βCD was reacted with 2-propargyloxynaphthalene and 2,7-dipropargyloxynaphthalene to obtain *mono*- and *bis*-NβCD respectively. To maximize the yield of *bis*-NβCD, the reaction was performed in two steps, the mono propargyloxynaphthalenyloxy-triazolyl βCD intermediate was isolated and the cycloaddition was repeated. Both products were isolated as a solid material, and chemical structures were confirmed by ^{1}H NMR, ^{13}C NMR and mass spectroscopy.

Model compound behaviour in solution and in the presence of βCD

Emission spectra for MON and dMON aqueous dilute solutions display single bands centred at ~347 nm and ~341, respectively, however the latter also presents a little shoulder around ~330 nm [Fig. 1S, ESI]. A decrease in medium polarity ($\varepsilon < 30$), by carrying out measurements in different polarity solvents, means that a shoulder appears at ~350 nm in the emission spectra and that there is a slight shift in the band for MON by about 3-4 nm to the blue. However, these changes are more evident in dMON, where a rather significant variation in the relative intensity of peak and shoulder takes place, without the occurrence of any band displacements (i.e. the initial high energy shoulder becomes a peak whose intensity increases upon polarity of the solvent decreasing [Fig. 2S,ESI]). Lifetimes,τ, for both compounds, obtained from the mono-exponential fluorescence intensity decay profiles as a function of solvent polarity, ε, are also depicted in Fig. 1S [ESI]. Both compounds behave similarly; τ varies little at $\varepsilon > 40$, it decreases when ε decreases in the $40 > \varepsilon > 30$ range and increases again at $\varepsilon < 30$. The latter is probably due to the viscosity increase in more apolar solvents (water and *n*-alcohols from methanol to heptanol). This behaviour is very similar to what is seen in some naphthalene carboxylates and dicarboxylates, which are used as polarity sensitive fluorescence probes.[11, 72]

Absorption spectra for model compounds in water exhibit bands centred at ~225 (232), ~272 (275) and ~323 (325) nm for MON (dMON), both in the absence and presence of native βCD. Bands displayed a slight intensity increase with [βCD]. The addition of βCD to a dilute MON aqueous solution exerts a shift on the location of the 347 nm peak fluorescence emission, due to changes in the polarity surrounding the guest, but also promotes the appearance of a shoulder around ~350 nm. For dMON, however, the intensity of the peak at ~341 relative to the shoulder at ~330 nm moderately increases upon βCD addition.

Decay intensity profiles in the presence of βCD were also resolved to mono-exponential functions. Lifetimes in the absence of βCD were 9.8 ns (10.1 ns) for MON (dMON) at 25ºC. However, as depicted in Fig. 3S [ESI], the MON model shows τ increasing with [βCD] while dMON lifetime decreases. The adjustments of experimental data to the conventional equations,[74] assuming a 1:1 stoichiometry complex, gave formation constants of 1050±80 M^{-1} and 645±84 M^{-1} at 25ºC for the MON and dMON binding to βCD respectively. There is an effective interaction with the βCD in both model compounds that results in the formation of stable complexes. However, whereas emission intensity almost appears to be unaffected by changes in polarity surrounding both guests upon complexation, lifetime is a suitable property with which to monitor the inclusion processes of both MON and dMON model compounds.

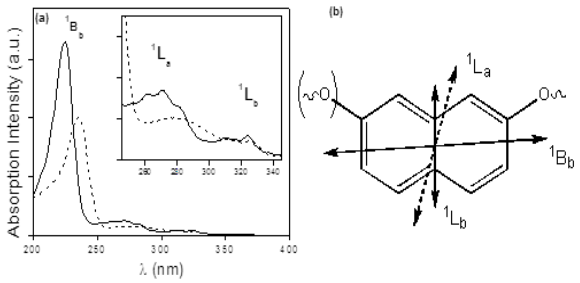

Fig. 2 (a) Absorption spectra at 25ºC of aqueous solution of *mono*-NβCD and *bis*-NβCD (dashed) at concentrations of 1.0×10^{-6} M and 1.7×10^{-6} M, respectively. (b) Orientation of the transition moments.

Fluorescence and Circular dichroism for *mono*- and *bis*-NβCDs in aqueous dilute solution

Fig. 2 shows absorption spectra for aqueous dilute solutions of *mono*- and *bis*-NβCDs. Bands for *mono*-NβCD are centred at ~325 and ~272 nm and a particularly intense band is observed at ~225 nm; molar absorptivities are 3400, 9500 and 132000 M^{-1}cm^{-1}, respectively. These bands are accompanied by shoulders (s) located at ~260, ~282 and ~310 nm. However, bands for *bis*-NβCD are placed at ~325 (s ~310 nm), ~280 nm and ~235 nm and molar absorptivities, smaller than for the *mono*-derivate, are 1600, 3400 and 35500 M^{-1}cm^{-1}, respectively. These bands are slightly shifted to the red by about 10-12 nm relative to the *mono*-NβCD. As in other naphthalene derivatives, [30] these bands can be ascribed to the $^{1}L_b$, $^{1}L_a$ and $^{1}B_b$ transitions, respectively. Transition moments are contained in the naphthalene ring plane and oriented along the main axis ($^{1}B_b$), the second perpendicular to it and along the minor axis ($^{1}L_b$) and the third forming a small angle with the previous one ($^{1}L_a$). Nevertheless, the value of the latter angle is uncertain as it depends on the substituent bound to the naphthalene group. For this reason some authors consider both moments as being oriented along the minor axis[30, 75-78]

Emission spectra are quite similar to their model compounds and show single bands with a maximum at ~345 nm for the *mono*-NβCD, whereas two peaks (~337 and ~348 nm) were found for the *bis*-NβCD [Fig. 4S, ESI]. No band shifts were observed upon increasing derivative concentration. The corrected fluorescence intensity [eq. 2 of Instruments and Experimental Methods] increased linearly with [*bis*-NβCD] in the whole concentration range used. Something similar occurred for the *mono*-NβCD.

However, the initial linearity observed disappeared at higher concentrations [Fig. 4S, ESI].

Fluorescence anisotropy (*r*) did not exhibit any noticeable variation with derivative concentration. Values of *r* were close to zero, but slightly larger for the *bis*-NβCD than the *mono*-derivative. Average values of *r* in the whole concentration range used were 0.0025±0.0010 and 0.0090±0.0017, respectively. Decay intensity profiles were, as models, always adjusted to mono-exponential decay functions. τ values were rather similar to those for their respective MON and dMON models and hardly exhibited any variation with *mono*- or *bis*-NβCD concentrations. Lifetime changes with temperature were in the ~9.4 ns (at 5 ºC) to ~8.2 ns (at 45 ºC) and ~11.7 ns (at 5 ºC) to ~10.7 ns (at 45 ºC) ranges for the *mono*- and *bis*-NβCD, respectively.

All fluorescence experiments, except for the change in emission intensity with [*mono*-NβCD], either indicates that there is no interaction between *mono*-NβCDs in the range of concentration used or that, if there is, changes in polarity and microviscosity surrounding this group during association hardly affect fluorescence properties. Our group has reported the self-association of quite similar cyclodextrin *mono*-derivatives whose appended groups were located on the macroring primary face and which contained diphenoxy groups instead of dinaphthoxy moieties. In addition, we have also reported the head-to-head association of modified CDs in aqueous media at the secondary side via a bidentate ligand which contains diphenoxy and naphthoxy groups. These non-covalent dimers which are stable in aqueous media dissociate in polar media.[10, 27, 28, 30, 79, 80]

On the other hand, circular dichroism (CD) spectra are able to provide information on the presence or absence of *mono*-NβCD association. The simple existence of the Cotton effect in the zone of chromophore absorption is unequivocal evidence of the interaction between the macroring appended naphthoxy group (ON) and its own cavity or a neighbouring one, providing information about its location and *mono*- or *bis*-derivative structure in solution.[81] Fig. 3 shows circular dichroism spectra for a dilute aqueous solution of the *mono*-NβCD and *bis*-NβCD at 25 ºC. The spectrum for the *mono*-NβCD exhibits weak positive ^1L_a and ^1L_b transition bands, whereas the zone for the ^1B_b transition shows a double signal whose maximum and minimum values are located at ~248 nm and ~222 nm, respectively. This bi-signal is accompanied by a little shoulder at ~232 nm, whereas the positive band seems to overlap the ^1L_a band. This combination of signs: positive, positive and negative for the ^1L_b y ^1L_a and ^1B_b transitions, respectively, would seem to correspond with a substituent arrangement by which the ON, located outside a CD cavity (or partially included), is oriented with the ^1B_b transition in the direction of the main CD axis and the other two, ^1L_b and ^1L_a, are perpendicular to it.

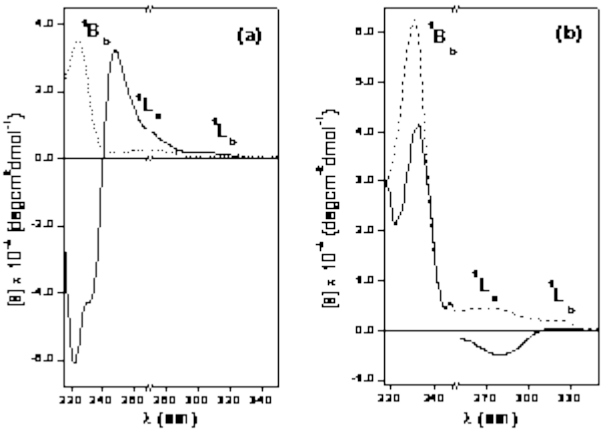

Fig. 3. Circular dichroism (—) and absorption spectra (---) of *mono*-NβCD (a) and *bis*-NβCD (b) aqueous dilute solutions at 25ºC. Concentrations were 10×10^{-6} M. Quartz cells were 10 mm paths for λ< 270 nm in (a) and λ< 250 nm in (b), and 100 mm paths for larger λ in both experiments.

As far as the region below 250 nm is concerned, the bi-signal that overlaps with ^1L_a and ^1B_b bands in the positive and negative components, respectively, may correspond, by symmetry and shape, to an exciton coupling (EC). This would imply that two chromophores, which absorb in this region, are rather close to each other and that at least one of them exhibits relatively large molar absorptivity. This may either be due to the interaction between two ON groups or between an ON group and a triazole one from the same substituent or different ones from two *mono*-NβCDs.

However, the circular dichroism spectrum for the *bis*-NβCD, which appears in Fig. 3 (b), exhibits positive dichroic signals, which are fairly intense for the ^1B_b band and extremely weak for ^1L_b and a low intensity negative signal for the ^1L_a transition. This combination of signs may correspond, "*a priori*", to an arrangement whereby the 2,7-dinaphthoxy (dON) chromophores which interact with a CD cavity are located outside any of them and oriented in such a manner that the ^1B_b transition moment is perpendicular to the main axis of one or both CDs, and the ^1L_a is parallel to this axis. The sign of the weak band would also appear not to be in disagreement with this arrangement due to its weakness and the uncertainty concerning the orientation of its transition moment.

Hetero-association of *mono*-NβCD with βCD

As Fig. 4 (a) shows, the single band observed at ~345 nm in the emission spectrum for the *mono*-NβCD aqueous solution becomes a double band, whose maxima are placed at ~340 and ~350 nm, upon βCD addition. These results, which are similar to observations of the complexation of MON and βCD, may be related to the fact that the ON group, in the presence of βCD, may be located in a more apolar medium, probably via interaction with the βCD cavity. Fluorescence decay profiles, carried out both in the absence and in the presence of βCD, were also fitted to mono-exponential functions. As depicted in 4 (b) at several temperatures, τ values increase with [βCD] up to a [βCD]/[*mono*-NβCD] molar ratio of ~100, where a near plateau is reached. Data can be adjusted to the proper equation for 1:1 stoichiometry complexes,[74] to provide binding constants that vary from 2020±350 M^{-1} at 5 ºC to 850±45 at 45 ºC [Table 1S collects binding constants at other temperatures, ESI]. Constants are very

similar to those reported for the complexation of some naphthalene dicarboxylates with *β*CD. [82]

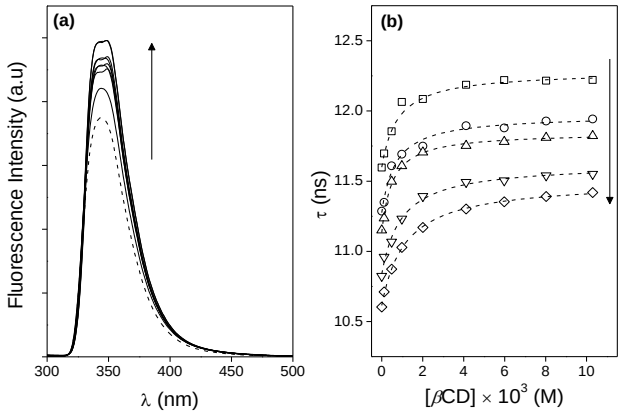

Fig. 4 (a) Emission spectra for *mono*-NβCD in the absence (---) and in the presence (—) of βCDs at different concentrations ([βCD]=0, 0.1, 0.5, 1.0, 2.0, 4.0, 6.0 8.0 and 10.3×10^{-3} M); (b) Fluorescence lifetime, τ, variation with βCD concentration at different temperatures; 5°C (□), 15 °C (○), 25 °C (△), 35 °C (▽) and 45 °C (◇). [*mono*-NβCD] was 10^{-5} M in all experiments.

Thermodynamics parameters, ΔH^0 and ΔS^0, have values of −18.1±1.0 kJmol^{-1} and −0.8 ±3.3 JK^{-1}mol^{-1}, respectively, and were obtained from linear van't Hoff plots [Fig. 5S, ESI]. Negative ΔH^0 values are related to the presence of favourable attractive, probably van der Waals host-guest interactions. Negative but close to zero entropy changes point to a probably partial inclusion into the cavity. The entropy gain due to ordered water loss does not offset the decrease in degrees of freedom caused by partial ON group inclusion to afford a favourable entropic term.

Influence of medium polarity on the association of *mono*-NβCD in solution

Emission spectra for dilute *mono*-NβCD solutions in water showed the typical single band centred at ~345 nm. However, a decrease in medium polarity caused two poorly defined peaks at ~350 and ~340 nm to appear [Fig. 6S, ESI]. A similar effect was observed during *mono*-NβCD heteroassociation with βCD and with the change of medium polarity and the complexation of model MON with βCD, *i.e.*, the guest entered into a more apolar cavity. Intensity decay profiles, monitored at 345 nm upon excitation at 279 nm, were again adjusted to monoexponential functions. Quantitative values of τ and their variation with solvent relative permittivity (ε) are depicted in Fig. 6S [ESI] and are very similar values for the free MON model compound.

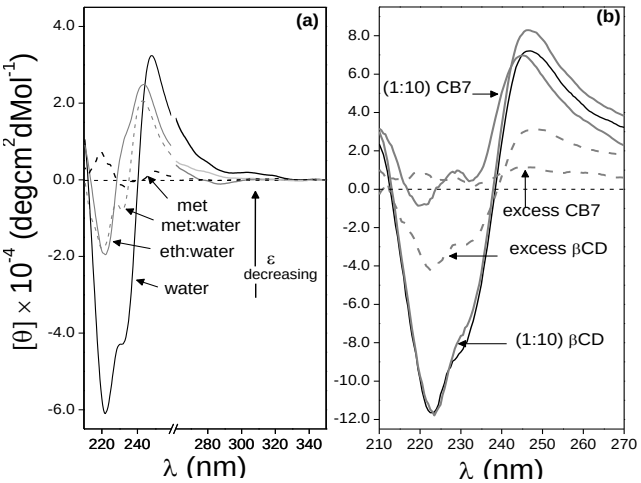

Fig. 5 Circular dichroism spectra for *mono*-NβCD (a) in water (solid black), methanol:water (1:1) (dashed gray) and ethanol:water (8:2) mixtures (solid gray) and methanol (dashed black); (b) *mono*-NβCD in the absence (solid black) and in the presence of βCD and CB7 at 1:10 molar ratios (solid gray) and a large excess of βCD and CB7 (dashed gray) at a fixed *mono*-NβCD concentration of 10^{-5} M.

Fig. 5 (a) shows ICD spectra for the dilute solution of the *mono*-NβCD in solvents of differing polarity. Signal intensity for the ^1B_b, ^1L_a and ^1L_b transitions, including the EC signal, decreases with decreasing solvent polarity. In fact, the ICD spectrum for the *mono*-NβCD disappears in methanol as a consequence of the rupture of possible *mono*-NβCD intermolecular associations in polar solvents.

Signs of ICD spectra for the *mono*-NβCD in water would appear to agree with the presence of tail-tail CD dimers where the ON group of one *mono*-derivate is *axially* oriented and partially included in neighbouring CDs via the primary face and *vice-versa*. Self -inclusion that would agree with the signs, in a way similar to CD *mono*derivatives containing phenoxy instead of naphthoxy groups, would be energetically unfavourable from the conformational point of view. [29] The presence of EC could be attributed to the monomeric form of the *mono*-NβCD, whose appended substituent is rather folded while the naphthoxy and triazole groups are relatively close together, but also to the previously stated tail-tail dimer, where the ON and triazole groups of neighbouring CDs are quite close. A non-polar medium would dissociate the dimer and probably extend the appended substituent chain in the monomeric form, decreasing both the EC signal.

A means to prove this statement can be found in capturing the substituent which contains the ON group of *mono*-NβCD monomers, to impede the approach of the ON-to-triazole group by adding other macrocycles, like the native natural βCD or CB7, to the water dilute solution of the *mono*-NβCD. These macrocycles should be able to favourably complex with *mono*-derivates and thus compete with dimerization. In fact, the feasibility of *mono*-NβCD hetero-association with the βCD has been quantitatively studied earlier in this paper.

Fig. 5 (b) shows ICD spectra in the EC zone from a dilute *mono*-NβCD solution in the presence of βCD, with which it forms a complex, or CB7, at 1:10 molar *mono*-NβCD:host ratios and at a large host excess. Hardly any shape or intensity changes take place in the circular dichroism spectrum upon the addition of βCD, up to a 1:10 ratio; however, an increase in the amount of βCD progressively translates into the disappearance of the induced signals. Although the equilibrium constant for the heteroassociation of the *mono*-NβCD and βCD, studied in the previous section, is not too large, the complexation process can favourably compete with dimer formation,

causing dissociation. This dissociation hardly occurred for CD *mono*-derivatives which contained diphenoxy groups instead of dinaphthoxy ones,[29] whose dimers seemed to be rather more stable. Adding βCD in that case barely displaced the dimer equilibrium toward the monomer form. In fact, it was necessary to add a strong competitor, an adamantane derivative, to dissociate it.[52, 83] The effect is more evident upon the addition of CB7 to the *mono*-NβCD solution and the intensity decreases faster than when using βCD. This would seem to agree with the occurrence of more efficient complexation between the appended ON group of the *mono*-NβCD and CB7, together with the fact that, due to the CB7 achirality, the *mono*-NβCD:CB7 complex should not show ICD signal. In fact the association constant for the heteroassociation of *mono*-NβCDs with CB7 was $1.9(\pm0.3)\times10^4$ M^{-1} at 25ºC [Fig. 7S, ESI].

Fluorescence quenching of *mono*- and *bis*-NβCD solutions

Quenching from fluorescence decay measurements at 25ºC on MON, dMON, *mono*-NβCD and *bis*-NβCD water dilute solutions were performed using the quencher, diacetyl (2,3-butanedione). Fig. 8S [ESI] depicts linear Stern-Volmer plots. Experiments were carried out on 10^{-5} M and 8×10^{-5} M *mono*-NβCD water solutions. Table 1 collects some of the parameters derived from these representations. Both model compounds show relatively large and very similar k_q values.

Table 1. Stern-Volmer constants ($K_{S\text{-}V}$), fluorescence lifetimes in the absence of diacetyl (τ_0) and bimolecular quenching constants (k_q).

System	$K_{S\text{-}V}$ (M^{-1})	τ_0 (ns)	$k_q\times10^9$ ($M^{-1}s^{-1}$)
MON	28.9 ± 0.7	9.7	3.0 ± 0.7
mono-NβCD (10^{-5} M)	17.6 ± 0.2	11.0	1.6 ± 0.2
mono-NβCD (8×10^{-5} M)	11.6 ± 0.5	11.6	1.0 ± 0.5
dMON	27.0 ± 0.6	10.1	2.7 ± 0.6
bis-NBCD	7.2 ± 0.1	8.4	0.9 ± 0.1

The *mono*-NβCD solution, 10^{-5} M, gave a k_q which is half that of the MON model. However, this value is larger than found for a *mono*-derivate solution whose concentration was 8×10^{-5} M (×8). A decrease in quencher accessibility to the ON group occurs upon dimer formation as the ON group is partially included in the βCD cavity. The dimer fraction should increase with [*mono*-NβCD]. The *bis*-NβCD solution, however, presents a k_q that is very similar to the one found for the *mono*-derivative at the highest concentration, probably due to the significant shielding of the chromophore group located between both CDs.

Molecular Dynamics simulations for isolated *mono*- and *bis*-NβCD

3 ns MD simulations were performed on isolated *mono*- and *bis*-derivatives structures depicted in Fig. 1 (see Computational protocols section). Averages of some of the more significant geometrical parameters obtained from the analysis of MD trajectories are collected in Table 3S [ESI]. For example, average distances throughout the trajectory between the βCD macroring and ON group centres of mass and between the ON and triazole groups centres of mass were 9.6±2.2 Å and 6.0±0.9 Å, respectively, for *mono*-NβCD. The average angles between the main βCD axis and the ^1L_a and ^1B_b transition moments for the ON group were 84±31 and 92±22º, respectively. Only conformations whose βCD-ON distances were smaller than 8 Å, *i.e.* those for which ON would in fact interact with the CD cavity, were considered for these calculations. 25% of the conformations fulfilled this condition, which explains the low intensity ICD spectra. Angle averages would appear to indicate that the ON plane is located almost perpendicularly to the main CD axis (parallel to the plane of CD bridging oxygen atoms), which would only explain the sign of the ^1L_a, but not the negative sign for the ^1B_b transition and the presence of EC in the ICD spectra, in *mono*-NβCD aqueous solutions.

As far as *bis*-NβCD is concerned, the centres of mass of both βCD macrorings are separated by an average distance of 13.2±2.6 Å, whereas the centre of mass of each CD and the dON group are placed at distances of 9.2±2.2 Å and 9.4±1.8 Å. The dON group never penetrates any of the CD cavities in any of the conformations and prefers to locate itself between the macrorings. The distances between the dON centre of mass and each triazole group were 5.8±0.9 and 6.0±1.0 Å, which are quite similar to those obtained for the *mono*-NβCD. This probably indicates that the EC signal, which appears in the *mono*-NβCD but not in the *bis*-NβCD, cannot be attributed to ON-triazole intramolecular interactions.

Angles for the main CD axis and ^1L_a and ^1B_b transition for the dON group were close to 90º for all of the four angles (Table 1S), which is in accordance with a geometrical arrangement in which the dON and bridging oxygen atoms planes are parallel. However, these results partially disagree with the combination of signs from the ICD spectra since they explain the positive sign for the ^1B_b transition but not the low negative intensity ^1L_a band. Nevertheless, the probability distribution for the ^1L_a-$CD_{main\ axis}$ angles are much wider than for the ^1B_b- $CD_{main\ axis}$, which would seem to indicate that there is a certain probability of finding conformations where the ^1L_a-$CD_{main\ axis}$ angles are smaller than 54.7º. 21% and 15% of the conformations fulfil this condition. The ^1L_a transition band in the circular dichroism spectra for this small number of conformations would be negative and the intensity, obviously, low.

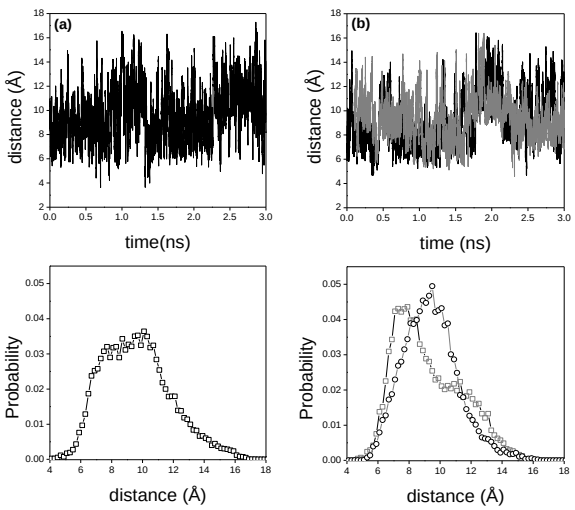

Fig. 6 (top panels): History of the CD-ON (—) distance for *mono*-NβCD (left) and the same for CD_1-dON (—) and CD_2-dON (—) distances for *bis*-NβCD (right). (bottom panels): Probability distributions for the CD-ON (-□-) (left), and CD_1-dON (-○-) and CD_2-dON (-□-) distances (right).

The top panels in Fig. 6 show the histories of the CD-ON distance for the *mono*-derivative and the CD_1-dON and CD_2-dON ones for the *bis*-derivative. No significant differences in the macroring centre to naphthoxy chromophore group distances, whose average values are

around 9-10Å, were found in either system. However, the probability distributions, depicted in the bottom panels of Fig. 6, are a little different. The distribution is relatively symmetric and centred at ~9 Å for *mono*-NβCD, whereas two rather different distributions were obtained for the two CD-dON distances in *bis*-NβCD. The CD_1-dON distance distribution is rather symmetric and centred at ~ 9-10 Å. However, the CD_2-dON distribution has two maxima located at ~7 and ~11 Å. These latter distributions describe two different arrangements: (*i*) the most probable, where both CD cavities are relatively close to the dON group making this group adopt a plane-parallel conformation relative to the CD plane of bridging oxygen atoms; (*ii*) where both CDs are more distant, the linker is relatively extended and the dON group tends to adopt orientations where the angles between the ^1L_a transition and any of the CD main axis are smaller than 54.7º. These conformations are responsible for the negative low intensity ^1L_a band observed in the *bis*-NβCD circular dichroism spectra. Concluding that the most plausible arrangements for *bis*-NβCD, which agree the experimental finding, are those in which the dinaphthoxy group laid in a quasi-parallel plane conformation between both CD macrorings [Fig. 9S, ESI].

Simulation for non-covalent (*mono*-NβCD)$_2$ dimers

MD simulations were also performed for two different non-covalent *mono*-NβCD dimer arrangements, TH and TT depicted in Fig. 7, in the presence of water. More details in the last section of this manuscript. The top of Fig. 8 depicts the optimized TH and TT starting structures for the MD simulations. Table 2S [ESI] brings together some of the geometrical and energetic parameters for both dimers. Fig. 8 shows histories for both CD macroring centres of mass, as well as for the total binding energies and contributions. The results show that TH dimers are not stable. Interaction energies throughout the trajectory are less favourable for the TH dimer than for the TT analogue, in fact they become zero at the end of the trajectory, indicating TH complex dissociation. However, the (*mono*-NβCD)$_2$ TT arrangement remains stable during and at the end of the MD trajectory. Van der Waals contributions are responsible for this stability. Fig. 9 depicts the TH and TT structures at the end of the MD trajectories.

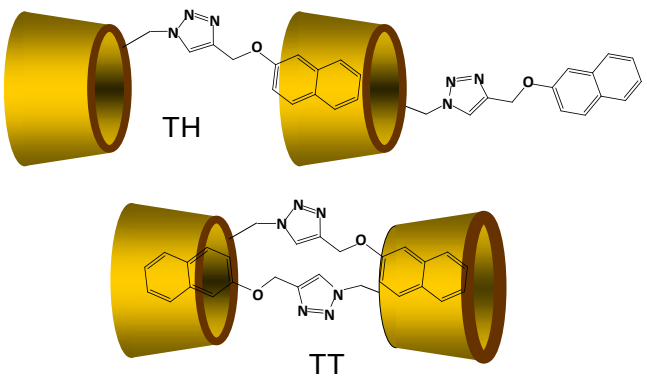

Fig. 7 TH and TT dimer (*mono*-NβCD)$_2$ arrangements used as starting conformations for MD simulations

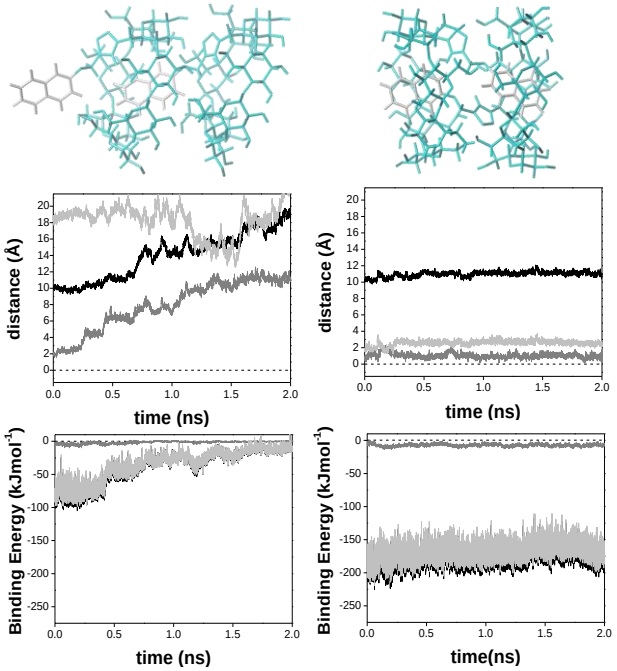

Fig. 8 (Top panel): Optimized non-covalent TH (left) and TT (right) (*mono*-NβCD)$_2$ dimers used as starting structures for MD. (Middle panels): Histories for the distances between CDs (black), ON1-CD2 (light gray) and ON2-CD1 (gray); and (bottom panels) for the total binding energies (black), electrostatics (gray) and van der Waals forces (light gray) for both the TH (left) and TT (right) arrangements.

Average angles between the main axis of each CD and the ^1B_b and ^1L_a transition moments for the TT dimer were close to 10º (31º) and 97º (72º) for the ON_1-CD_2 (ON_2-CD_1) interactions. In addition, CD_1-ON_2 and CD_2-ON_1 distance averages of ~1.0 and 2.6 Å, respectively, indicate that at least one of the ON groups is close but slightly outside the CD cavity. Angles between the CD axis and ^1B_b and ^1L_a transition moments for each CD show the presence of conformations where *axially* oriented ON groups are located outside the neighbouring CD cavity. These conformations would appear to agree with the negative and positive signs observed in the circular dichroism spectra for the ^1B_b and ^1L_a bands of *mono*-NβCD and also with the presence of the excitonic coupling signal observed in *mono*-NβCD, but not for *bis*-NβCD. Table 2S [ESI] shows the average TT dimer distances between each ON group and the triazole from the neighbouring CD, which in some cases is smaller than ~5 Å. This distance is short enough to provide an interaction that is favourable for EC. The circular dichroism spectra could never be explained without the presence of these TT dimers. Unfortunately, the low solubility of these compounds makes it impossible to use NMR techniques to further prove the presence of these dimeric structures.

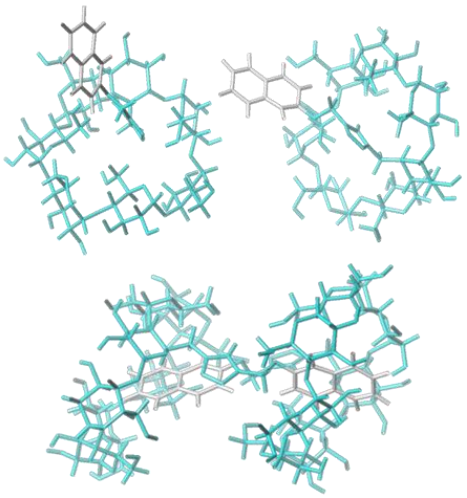

Fig. 9 Structures for the TH (top) and TT (bottom) arrangements for (*mono*-NβCD)$_2$ dimers at the end of 2ns MD trajectories.

Conclusions

The aqueous solution structures of *mono*- and *bis*-βciclodextrin derivatives (*mono*- and *bis*-NβCDs) that contain dinaphthoxy groups, either as appended moieties or inter-CD linkers, have been predicted using fluorescence and circular dichroism spectroscopy and molecular dynamics simulations. Absorption spectra for model compounds, *mono*- and *bis*-βCD derivatives, exhibit typical naphthoxy bands which originate from the ^1B_b, ^1L_a and ^1L_b transitions. Emission spectra for *mono*- and *bis*-βCD derivatives show characteristics that are similar to their corresponding model compounds. Fluorescence anisotropy and lifetimes measurements are hardly sensitivity to changes in the microenvironment surrounding the naphthoxy chromophore. However, an analysis of the circular dichroism spectra for *mono*-NβCD, in media of differing polarity and in the presence of other macrorings, supported molecular dynamics simulations and confirmed that *mono*-NβCD forms stable tail-to-tail dimers via the partial *axial* interpenetration of naphthoxy groups from the appended moiety into the primary faces of their neighbouring CDs. Dimers also explain the presence of an exciton coupling ICD signal, which is caused by intermolecular interactions between naphthoxy and triazole groups from neighbouring CDs. There was no EC signal in the ICD spectra for the *bis*-NβCD. The dinaphthoxy unit in the aqueous solution *bis*-NβCD linker is located between the CDs in a quasi parallel-plane arrangement with respect to the bridging βCD oxygen atoms and the dinaphthoxy group long (minor) axis is perpendicular (forming an angle smaller than 54.7º) to the main βCD axis direction.

It has been demonstrated that the hydrophobic nature of the appended *mono*-NβCD naphthalene moiety promotes the formation of relatively stable dimeric supramolecular structures in aqueous solution. These structures partially block the primary or secondary faces of the cyclodextrin cavities and thus compete with the complexation of any guest molecule. On the other hand, the aqueous solution *bis*-derivatives present an arrangement where the cavities of both macrorings remain free and are therefore capable of accommodating molecule guests between or inside their cavities. The complexation of bis-NβCD adducts containing Gd(III) chelates will be part of future work.

Experimental and theoretical protocols

Materials and Methods

Synthesis, Reagents and Solutions. Commercially available reagents and solvents for the syntheses were used without further purification. Native CDs were kindly provided by Wacker Chemie. Reactions under combined MW/US irradiation were performed in a professional multimode oven, (Microsynth, Milestone), operating at 2.45 GHz, equipped with a high-power pyrex® US probe (20.5 kHz working frequency), while temperature was strictly monitored by a fibre optic thermometer inside the reaction vessel.

Commercial 2-metiloxynaphtalene, MON and 2,7-dimethoxynaphthalene, dMON (Aldrich, ≥ 98 %) were used as model compounds for *mono*- and *bis*-NβCDs respectively. They were checked using fluorescence and then used without any further purification. Native βCD was purchased from Aldrich and a Karl-Fischer analysis revealed that it contained a water content of 12.94 %. Cucurbituril of seven glicouril units, CB7 (Aldrich, water content 22.1%) were used without further purification. 2,3-Butanedione ($C_4H_6O_2$, diacetyl, Aldrich) was used as a fluorescence quencher for the naphthoxy group. Solvents were: deionised *milli*-Q water, linear *n*-alcohols from methanol to *n*-heptanol (Aldrich spectrophotometric grade or purity >98%).

Mono- and *bis*-derivatives of β-cyclodextrin, 6^I-deoxy-6^I-(4-((2-naphthyloxy)methyl)-1*H*-1,2,3-triazol-1-yl)-β-cyclodextrin and 2,7-bis-((1-(6^I-deoxy-β-cyclodextrin-6^I-yl)-1*H*-1,2,3-triazol-4-yl)methoxy)naphthalene, named *mono*- and *bis*-NβCD respectively, are depicted in Fig. 1. The syntheses were carried out via CuAAC using metallic copper under sonochemical conditions.[74]

*Synthesis of 6^I-deoxy-6^I-(4-((2-naphthyloxy)methyl)-1H-1,2,3-triazol-1-yl)-β-cyclodextrin (mono-*NβCD*).* β-naphthol (400 mg, 2.78 mmol, 1 eq) was dissolved in 10 ml of acetone and K_2CO_3 (1.53 g, 11.12 mmol, 4 eq) was added to the solution. The mixture was kept at 70°C for 30 min under magnetic stirring. Then, propargyl bromide (360 µl, 3.34 mmol, 1.2 eq) was added and the reaction was left at 70°C for 4 h. The crude product was extracted using CH_2Cl_2 and then purified on silica gel. 126 mg of the pure product (0.690 mmol, 4 eq) were reacted with 6^I-azido-6^I-deoxy-β-CD (200 mg, 0.172 mmol, 1 eq) in 10 ml of DMF in the presence of 100 mg of Cu. The reaction was carried out under combined MW/US irradiation at 100°C for 1.5 h. The copper was filtered off and the crude product was precipitated in a water/acetone mixture and then purified on RP18. 173 mg of pure product were obtained (0.129 mmol, 75%). Scheme and more details in the ESI.

Synthesis of 2,7-bis-((1-(6^I-deoxy-β-cyclodextrin-6^I-yl)-1H-1,2,3-triazol-4-yl)methoxy) naphthalene (bis-NβCD). 2,7-dihydroxynaphthalene (1 g, 6.24 mmol, 1 equiv) was dissolved in acetone (15 ml) and K_2CO_3 (6.89 g, 49.9 mmol, 8 equiv) was added to the solution. The mixture was kept at 70°C for 30 min under magnetic stirring. Then, propargyl bromide (1.62 ml, 14.98 mmol, 2.4 equiv) was added and the reaction was left at 70°C for 4 h. The crude product was extra**cted** using CH_2Cl_2 and then purified on silica gel obtaining 865 mg of pure product (3.66 mmol, 59% yield). 2,7-dipropargyloxynaphtalene (244 mg, 1.033 mmol, 3 equiv) was reacted with 6^I-azido-6^I-deoxy-β-CD (400 mg, 0.345 mmol, 1 equiv) in DMF (10 ml) in the presence of metallic copper powder (200 mg). The reaction was carried

out under combined MW/US irradiation at 100°C for 1.5 h. The copper was filtered off and the crude product was precipitated in a water/acetone mixture then purified on RP18. 458.4 mg of 6^Ideoxy-6^I-(4-((7-propargyloxynaphthalen-2-yloxy)methyl)-1H-1,2,3-triazol-1-yl)-β-CD (0.328 mmol, 76% yield) and pure 2,7-bis-((1-(6^I-deoxy-β-cyclodextrin-6^I-yl)-1H-1,2,3-triazol-4-yl)methoxy)naphthalene (bis-NβCD) (70 mg, 0.0274 mmol, yield 13%) was isolated. In order to increase the dimer yield, the same synthetic procedure was repeated on 0.150 mg of 6^I-azido-6^I-deoxy-β-CD (0.129 mmol, 1 equiv) and 180 mg of 6^I-deoxy-6^I-(4-((7-propargyloxynaphthalen-2-yloxy)methyl)-1H-1,2,3-triazol-1-yl)-β-CD (0.129 mmol, 1 equiv). In this case, after purification the bis-NβCD was recovered with a 28% yield (92 mg, 0.036 mmol).

Instruments and Experimental Methods. Absorption spectra were obtained by using a Perkin-Elmer Lambda-35 Spectrometer. Steady-state fluorescence and time-resolved measurements were performed on SLM 8100 AMINCO and TCSPC FL900 Edinburgh Instruments spectrofluorometers. Characteristics and measurement conditions have been previously described[10, 28, 30, 80]. Excitation for the time-resolved measurements was carried out using sub-nanosecond pulsed NanoLED (IBH), emitting at 279 nm. Data acquisition was performed on 1024 channels at a time window width of 200 ns with a total of 10,000 counts measured at the maximum of the intensity profile. Samples were held at a constant temperature by two Huber Ministat baths in both instruments. Right angle geometry and magic angle (for steady-state) conditions were used. Decay intensity profiles were fitted to a sum of exponential decay functions by the iterative reconvolution method.[84] The intensity weighted average lifetime of a multiple-exponential decay function was then defined as,[85]

$$\langle \tau \rangle = \frac{\sum_{i=1}^{n} A_i \tau_i^2}{\sum_{i=1}^{n} A_i \tau_i} \qquad (1)$$

where A_i is the pre-exponential factor of the component and τ_i is the lifetime of the multi-exponential function intensity decay. Corrections due to the inner effect, which is only significant at the highest concentrations, were made,[86]

$$I_{corr} = I_{obs}\ antilog\left(\frac{A_{ex} + A_{em}}{2}\right) \qquad (2)$$

where A_{ex} and A_{em} are the absorption at the wavelength of excitation and emission respectively.
Induced Circular Dichroism (ICD) spectra were obtained using a JASCO J-715 spectropolarimeter. Recorded spectra were the average of three scans taken at a speed of 20 nm min^{-1} with a time response of 0.125 s. In order to maintain the absorbance around 1 at the maximum of the selected absorption band, several quartz cell paths (from 1 to 100 mm) were used. The sensitivity and resolution were set at 20 mdeg and 0.5 nm respectively. Measurements were performed at 25°C.

Computational Protocols. Conformational studies on isolated *mono*- and *bis*-NβCDs were performed on the analysis of the 3ns Molecular Dynamics simulations (MD) in vacuum using Sybyl-X2.0[87] and the Tripos Force Field.[88] The potential energy of each system was evaluated as the sum of bond stretching, bond angle bending, torsional, van der Waals, electrostatic and out of plane energy contributions. A relative permittivity of ε=1 was used. Partial atomic charges were calculated using MOPAC and an AM1 Hamiltonian by separately obtaining charges for the CDs and for the appended group or spacer (in the all *trans* conformation).[89] Charges for the MON and dMON model compounds were obtained using the same method. Optimization was carried out using the simplex algorithm, and the conjugate gradient was used as the termination method with gradients of 0.05 Kcal/mol.[90] Non-bonded cut-off distances were set at 8 Å. The 3ns MD trajectories were performed on the optimized all *trans* (for the appended group or spacer) and non-distorted (for the macro-ring) *mono*- and *bis*-derivative structures at 500K following procedures described elsewhere.[29] Conformations were saved every 200 fs, yielding 15,000 images per trajectory for subsequent analysis. The average of any property was calculated by equally weighing each image.
The structures of (*mono*-NβCD)$_2$ dimers, however, were studied on the basis of 2 ns MD trajectory analyses in water on two initial minimized tail-to-head (TH) and tail-to-tail (TT) arrangements, represented in Fig. 7 and 8. In these two structures, the *axially* oriented naphthoxy group of one CD either enters its CD partner via the secondary face (TH), or the *axially* oriented naphthoxy groups of each CD penetrates its neighbouring CD via the primary face and *vice versa* (TT). MD simulations were performed on each of the minimized (gradient 0.5 kcal/molÅ), solvated TH and TT arrangements (PBC, Silverware algorithm).[91] MD characteristics were similar to those used in other dimerization processes,[29] *i.e.*, an equilibration period of 25 ps, integration time step of 2 fs and velocities rescaled at 100 fs intervals. Bonds containing H atoms were constrained to not vibrating during the entire trajectory, which consisted of 8,000 images, as data were saved every 250 fs.

Acknowledgements

This work was supported by the University of Turin (fondi ricerca locale 2013, ex-60%) and the Universidad de Alcalá (GC2011-002 and UAH2011/EXP-036). TC acknowledges FPI predoctoral fellowship from Spanish MICINN. FM and TC recognize the assistance of M.L. Heijnen with the preparation of the manuscript.

REFERENCES

1. H. Dodziuk and Editor, *Cyclodextrins and Their Complexes*, Wiley-VCH Verlag GmbH & Co. KGaA, 2008.
2. F. Davis and S. Higson, in *Macrocycles: Construction, Chemistry and Nanotechnology Applications*, John Wiley & Sons, Chichester, 2011, pp. 190-254.
3. A. Douhal, *Cyclodextrins Materials, Photochemistry, Photophysics and Photobiology*, Elsevier, Amsterdam, 2006.
4. J. M. Madrid, M. Villafruela, R. Serrano and F. Mendicuti, *J. Phys. Chem. B*, 1999, **103**, 4847-4853.
5. P. R. Sainz-Rozas, J. R. Isasi and G. Gonzalez-Gaitano, *J. Photochem. Photobiol., A*, 2005, **173**, 319-327.
6. A. Di Marino and F. Mendicuti, *Appl. Spectrosc.*, 2004, **58**, 823-830.
7. I. Pastor, A. Di Marino and F. Mendicuti, *J. Photochem. Photobiol., A*, 2005, **173**, 238-247.
8. A. Di Marino and F. Mendicuti, *Appl. Spectrosc.*, 2002, **56**, 1579-1587.
9. J. A. B. Ferreira and S. M. B. Costa, *J. Photochem. Photobiol., A*, 2005, **173**, 309-318.

10. M. J. González-Álvarez, A. Di Marino and F. Mendicuti, *J. Fluoresc.*, 2009, **19**, 449-462.
11. F. Mendicuti, *Trends Phys. Chem.*, 2006, **11**, 61-77.
12. A. Ueno, S. Minato, I. Suzuki, M. Fukushima, M. Ohkubo, T. Osa, F. Hamada and K. Murai, *Chem. Lett.*, 1990, **19**, 605-608.
13. M. N. Berberan-Santos, J. Canceill, J. C. Brochon, L. Jullien, J. M. Lehn, J. Pouget, P. Tauc and B. Valeur, *J. Am. Chem. Soc.*, 1992, **114**, 6427-6436.
14. M. N. Berberan-Santos, J. Pouget, B. Valeur, J. Canceill, L. Jullien and J. M. Lehn, *J. Phys. Chem.*, 1993, **97**, 11376-11379.
15. K. Hamasaki, H. Ikeda, A. Nakamura, A. Ueno, F. Toda, I. Suzuki and T. Osa, *J. Am. Chem. Soc.*, 1993, **115**, 5035-5040.
16. D. M. Gravett and J. E. Guillet, *J. Am. Chem. Soc.*, 1993, **115**, 5970-5974.
17. L. Jullien, J. Canceill, B. Valeur, E. Bardez and J.-M. Lehn, *Angew. Chem., Int. Ed.*, 1994, **106**, 2582-2584.
18. Y. Wang, T. Ikeda, H. Ikeda, A. Ueno and F. Toda, *Bull. Chem. Soc. Jpn.*, 1994, **67**, 1598-1607.
19. H. Ikeda, M. Nakamura, N. Ise, N. Oguma, A. Nakamura, T. Ikeda, F. Toda and A. Ueno, *J. Am. Chem. Soc.*, 1996, **118**, 10980-10988.
20. H. Ikeda, M. Nakamura, N. Ise, F. Toda and A. Ueno, *J. Org. Chem.*, 1997, **62**, 1411-1418.
21. T. Ikunaga, H. Ikeda and A. Ueno, *Chem.-Eur. J.*, 1999, **5**, 2698-2704.
22. M. N. Berberan-Santos, P. Choppinet, A. Fedorov, L. Jullien and B. Valeur, *J. Am. Chem. Soc.*, 1999, **121**, 2526-2533.
23. T. Aoyagi, H. Ikeda and A. Ueno, *Bull. Chem. Soc. Jpn.*, 2001, **74**, 157-164.
24. J. W. Park, H. E. Song and S. Y. Lee, *J. Phys. Chem. B*, 2002, **106**, 7186-7192.
25. J. W. Park, S. Y. Lee and S. M. Kim, *J. Photochem. Photobiol., A*, 2005, **173**, 271-278.
26. H. Ikeda, T. Murayama and A. Ueno, *Org. Biomol. Chem.*, 2005, **3**, 4262-4267.
27. P. Balbuena, D. Lesur, M. J. G. Alvarez, F. Mendicuti, C. O. Mellet and J. M. G. Fernandez, *Chem. Commun.*, 2007, 3270-3272.
28. M. J. González-Álvarez, P. Balbuena, C. Ortiz Mellet, J. M. García Fernández and F. Mendicuti, *J. Phys. Chem. B*, 2008, **112**, 13717-13729.
29. T. Carmona, M. J. Gonzalez-Alvarez, F. Mendicuti, S. Tagliapietra, K. Martina and G. Cravotto, *J. Phys. Chem. C*, 2010, **114**, 22431-22440.
30. M. J. González-Álvarez, J. M. Benito, J. M. García Fernández, C. Ortiz Mellet and F. Mendicuti, *J. Phys. Chem. B*, 2013, **117**, 5472-5485.
31. R. Freeman, T. Finder, L. Bahshi and I. Willner, *Nano Lett.*, 2009, **9**, 2073-2076.
32. R. Krishnaveni, P. Ramamurthy, M. E. J. Padma and P. Divya, *J. Photochem. Photobiol., A*, 2012, **229**, 60-68.
33. G. Fang, M. Xu, F. Zeng and S. Wu, *Langmuir*, 2010, **26**, 17764-17771.
34. M. Toda, Y. Kondo and F. Hamada, *J. Incl. Phenom. Macrocycl. Chem.* , 2007, **59**, 341-344.
35. L. Li, C.-F. Ke, H.-Y. Zhang and Y. Liu, *J. Org. Chem.*, 2010, **75**, 6673-6676.
36. G. Fukuhara, T. Mori and Y. Inoue, *J. Org. Chem.*, 2009, **74**, 6714-6727.
37. T. Kikuchi, M. Narita and F. Hamada, *Tetrahedron*, 2001, **57**, 9317-9324.
38. Y. Liu, J. Shi and D.-S. Guo, *J. Org. Chem.*, 2007, **72**, 8227-8234.
39. H. Nakashima and N. Yoshida, *Org. Lett.*, 2006, **8**, 4997-5000.
40. Y. Liu, Y. Chen, B. Li, T. Wada and Y. Inoue, *Chem.-Eur. J.*, 2001, **7**, 2528-2535.
41. Y. Liu, C. C. You and B. Li, *Chem.-Eur. J.*, 2001, **7**, 1281-1288.
42. D. Rong and V. T. D'Souza, *Tetrahedron Lett.*, 1990, **31**, 4275-4278.
43. Y. Liu, Y. Chen, L. Li, H.-Y. Zhang, S.-X. Liu and X.-D. Guan, *J. Org. Chem.*, 2001, **66**, 8518-8527.
44. S. Filippone, F. Heimann and A. Rassat, *Chem. Commun.*, 2002, 1508-1509.
45. H. F. M. Nelissen, M. C. Feiters and R. J. M. Nolte, *J. Org. Chem.*, 2002, 5901-5906.
46. D.-Q. Yuan, J. Lu, M. Atsumi, A. Izuka, M. Kai and K. Fujita, *Chem. Commun.*, 2002, 730-731.
47. Y. Liu, L. Li, H.-Y. Zhang and Y. Song, *J. Org. Chem.*, 2003, **68**, 527-536.
48. Y. Liu, Y. Song, H. Wang, H.-Y. Zhang, T. Wada and Y. Inoue, *J. Org. Chem.*, 2003, **68**, 3687-3690.
49. T. Lecourt, J.-M. Mallet and P. P. Sinay, *Eur. J. Org. Chem.*, 2003, 4553-4560.
50. S. Filippone and A. Rassat, *C. R. Chim.*, 2003, **6**, 83-86.
51. Y. Liu, H. Wang, P. Liang and H.-Y. Zhang, *Angew. Chem., Int. Ed.*, 2004, **43**, 2690-2694.
52. Y. Liu, X.-Q. Li, Y. Chen and X.-D. Guan, *J. Phys. Chem. B*, 2004, **108**, 19541-19549.
53. Y. Liu, Y. Song, Y. Chen, X.-Q. Li, F. Ding and R.-Q. Zhong, *Chem.-Eur. J.*, 2004, **10**, 3685-3696.
54. J. Yang, Y. Wang, A. Rassat, Y. Zhang and P. Sinay, *Tetrahedron*, 2004, **60**, 12163-12168.
55. K.-R. Wang, D.-S. Guo, B.-P. Jiang, Z.-H. Sun and Y. Liu, *J. Phys. Chem. B*, 2010, **114**, 101-106.
56. Y.-M. Zhang, Y. Chen, Y. Yang, P. Liu and Y. Liu, *Chem.-Eur. J.*, 2009, **15**, 11333-11340.
57. Y. Liu, L. Li, H.-Y. Zhang, Y.-W. Yang and F. Ding, *Supramol. Chem.*, 2004, **16**, 371-379.
58. Y. Liu, Y.-L. Zhao, Y. Chen, F. Ding and G.-S. Chen, *Bioconjugate Chem.*, 2004, **15**, 1236-1245.
59. Y. Liu, Y.-L. Zhao, Y. Chen, P. Liang and L. Li, *Tetrahedron Lett.*, 2005, **46**, 2507-2511.
60. Y. Liu, H. Wang, Y. Chen, C.-F. Ke and M. Liu, *J. Am. Chem. Soc.*, 2005, **127**, 657-666.
61. Y. Liu, Y. Song, Y. Chen, Z.-X. Yang and F. Ding, *J. Phys. Chem. B*, 2005, **109**, 10717-10726.
62. Y. Liu, P. Liang, Y. Chen, Y.-L. Zhao, F. Ding and A. Yu, *J. Phys. Chem. B*, 2005, **109**, 23739-23744.
63. Y. Liu, S. Kang, Y. Chen, R. Cao and J. Shi, *Comb. Chem. High Throughput Screening*, 2007, **10**, 350-357.
64. S. Aime, E. Gianolio, G. Palmisano, B. Robaldo, A. Barge, L. Boffa and G. Cravotto, *Org. Biomol. Chem.*, 2006, **4**, 1124-1130.
65. K. Yamauchi, Y. Takashima, A. Hashidzume, H. Yamaguchi and A. Harada, *J. Am. Chem. Soc.*, 2008, **130**, 5024-5025.
66. Y. Liu, Z. Fan, H.-Y. Zhang, Y.-W. Yang, F. Ding, S.-X. Liu, X. Wu, T. Wada and Y. Inoue, *J. Org. Chem.*, 2003, **68**, 8345-8352.

67. Y. Liu, H.-X. Wu, Y. Chen and G.-S. Chen, *Supramol. Chem.*, 2009, **21**, 409-415.
68. T. Carmona, N. Mayordomo, K. Martina, G. Cravotto and F. Mendicuti, *J. Photochem. Photobiol., A*, 2012, **237**, 38-48.
69. A. Barge, M. Caporaso, G. Cravotto, K. Martina, P. Tosco, S. Aime, C. Carrera, E. Gianolio, G. Pariani and D. Corpillo, *Chem, - Eur. J.*, 2013, **19**, 12086-12092.
70. G. Cravotto, F. Mendicuti, K. Martina, S. Tagliapietra, B. Robaldo and A. Barge, *Synlett*, 2008, **17**, 2642-2646.
71. S. Aime, E. Gianolio, F. Arena, A. Barge, K. Martina, G. Heropoulos and G. Cravotto, *Org. Biomol. Chem.*, 2009, **7**, 370-379.
72. M. Cervero and F. Mendicuti, *J. Phys. Chem. B*, 2000, **104**, 1572-1580.
73. P. Cintas, A. Barge, S. Tagliapietra, L. Boffa and G. Cravotto, *Nature Prot.*, 2010, **5**, 607-616.
74. R. Usero, C. Alvariza, M. J. González-Álvarez and F. Mendicuti, *J. Fluoresc.*, 2008, **18**, 1103-1114.
75. M. Kodaka, *J. Phys. Chem.*, 1991, **95**, 2110-2112.
76. M. Kodaka, *J. Am. Chem. Soc.*, 1993, **115**, 3702-3705.
77. M. Kodaka, *J. Chem. Soc., Faraday Trans.*, 1997, **93**, 2057-2059.
78. M. Kodaka, *J. Phys. Chem. A*, 1998, **102**, 8101-8103.
79. M. J. González-Álvarez, N. Mayordomo, L. Gallego-Yerga, C. O. Mellet and F. Mendicuti, *Tetrahedron*, 2012, **68**, 2961-2972.
80. M. J. González-Álvarez, A. Méndez-Ardoy, J. M. Benito, J. M. García Fernández and F. Mendicuti, *J. Photochem. Photobiol., A*, 2011, **223**, 25−36.
81. N. Berova, K. Nakanishi and R. W. Woody, *Circular Dichroism: Principles and Applications*, Wiley-VCH, 2000.
82. S. Hamai, *Bull. Chem. Soc. Jpn.*, 2010, **83**, 1489-1500.
83. Y. Song, Y. Chen and Y. Liu, *J. Photochem. Photobiol., A*, 2005, **173**, 328-333.
84. D. V. O'Connor, W. R. Ware and J. C. Andre, *J. Phys. Chem. B*, 1979, **83**, 1333-1343.
85. J. R. Lakowicz, in *Principles of Fluorescence Spectroscopy*, Springer, New York, 3rd edn., 2006, p. 97.
86. J. R. Lakowicz, in *Principles of Fluorescence Spectroscopy*, Springer, New York, 3rd edn., 2006, p. 56.
87. (2013) SybylX 2.0, Tripos International, 1699 S Hanley Road, St Louis, MO, 63144 USA.
88. M. Clark, R. D. Cramer, III and O. N. Van, *J. Comput. Chem.*, 1989, **10**, 982-1012.
89. MOPAC(AM1), (Included in the Sybyl X2.0 package.).
90. Y. Brunel, H. Faucher, D. Gagnaire and A. Rassat, *Tetrahedron*, 1975, **31**, 1075-1091.
91. M. Blanco, *J. Comput. Chem.*, 1991, **12**, 237-247.